AD NUMBER

AD845302

LIMITATION CHANGES

TO:

Approved for public release; distribution is unlimited.

FROM:

**Distribution authorized to U.S. Gov't. agencies and their contractors;
Administrative/Operational Use; 16 DEC 1968.
Other requests shall be referred to Director, Defense Advanced Research Projects Agency, 3701 N. Fairfax Dr., Arlington, VA 22203- 1714.**

AUTHORITY

USAF ltr 5 Jan 1972

TR 68-51

AD845302

TECHNICAL REPORT NO. 68-51

PRELIMINARY EVALUATION OF THE UBSO VERTICAL ARRAY

attn: VELA Seismol. Ctr.
Wash DC 20333

GEOTECH
A TELEDYNE COMPANY

40

TECHNICAL REPORT NO. 68-51

PRELIMINARY EVALUATION OF THE UBSO VERTICAL ARRAY

by

Dale S. Kelley

Sponsored by

Advanced Research Projects Agency
Nuclear Test Detection Office
ARPA Order No. 624

GEOTECH
A TELEDYNE COMPANY
3401 Shiloh Road
Garland, Texas

16 December 1968

IDENTIFICATION

AFTAC Project No. VELA T/6705
Project Title: Operation of UBSO
ARPA Order No. 624
ARPA Program Code No. 6F10
Name of Contractor: Teledyne Industries, Geotech Division
Garland, Texas
Date of Contract: 1 May 1966

Amount of Contract and Amendment 1:	$ 624,897
Amount of Amendment 2:	$ 374,600
Contract Change Notice No. 1	$ 144,173
Amount of Supplemental Agreement No. 5	$ 59,322
Amount of Supplemental Agreement No. 6 (negotiated not executed)	$ 36,257
Total:	$1,239,249

Contract No. AF 33(657)-16563
Contract Expiration Date: 31 December 1968
Program Manager: B. B. Leichliter, BR1-2561, Ext. 222

CONTENTS

ILLUSTRATIONS

TABLES

ABSTRACT

The vertical array at the Uinta Basin Seismological Observatory consists of six short-period seismographs distributed along the 9000-foot depth of the Carter U.S. No. 1 well. A study of four data samples containing teleseismic earthquake signals indicated a maximum improvement of about 9 dB in signal-to-noise ratio of a single vertical array instrument to a surface instrument. Analyses of two noise samples indicate that the noise field consists of fundamental mode Rayleigh waves for periods greater than 2.5 seconds, at shorter periods the noise field is primarily dominated by P-wave noise.

PRELIMINARY EVALUTION OF THE UBSO VERTICAL ARRAY

1. INTRODUCTION

1.1 AUTHORITY

The work described in this report was supported by the Advanced Research Projects Agency, Nuclear Test Detection Office, and was monitored by the Air Force Technical Applications Center (AFTAC), under Contract AF 33(657)-16563.

1.2 HISTORY

To provide data with which a comparison of the effectiveness of a vertical array of short-period seismographs and a more conventional near-surface array of short-period seismographs could be made, a 6-element array of vertical seismographs was installed at UBSO during the first 6 months of Project VT/6705. Installation was completed on 5 September 1966, and the array was operated until July 1967, when an accumulation of equipment malfunctions caused the Project Officer to instruct UBSO personnel to suspend operations. The array was reinstalled in February 1968, and has been operating intermittently since that time. The data samples used in this preliminary study were selected during operational periods of the array in the springs of 1967 and 1968.

1.3 PURPOSE OF THE INVESTIGATION

The reliability of the UBSO vertical array instrumentation system has not been adequate to provide data suitable for a comprehensive noise study; consequently, the purpose of this report is to provide a preliminary noise analysis based on a few data samples obtained during periods when the vertical array was known to be operating reliably.

A proposal to retrofit the vertical array by replacing the obsolete equipment and increasing the number of sensors in the well is currently pending. The retrofit of the array will permit a comprehensive study of the noise field and a comparison of the detection capabilities of the vertical and the shallow-buried arrays.

The principal areas of investigation in this study are the determination of signal and noise amplitudes as a function of depth; determination of the principal components of the ambient noise field; and the computation of signal-to-noise ratios (S/N) for individual elements and summations of the vertical and shallow-buried arrays.

2. OPERATIONAL PARAMETERS

2.1 VERTICAL ARRAY

2.1.1 Geological Environment

Situated near the eastern end of the east-west axis of the Uinta Basin, the UBSO vertical array penetrates a continuous section of low-velocity sediments of tertiary age. It commences in the Duchesne River formation and reaches its total depth of 2745 meters (9007 feet) in the Wasatch formation. Figure 1 shows the position of the array in a hypothetical cross section. A lithologic log was constructed from formation cuttings and cores when the hole was drilled, and sonic-velocity and density logs were made when the hole was prepared for the installation of seismometers. Data from these logs have been combined in figure 2 which shows the stratigraphy, the velocities, and the densities of the formations underlying UBSO.

2.1.2 Instrumentation and System Response

The vertical array consists of six deep-hole, short-period seismometers, Geotech Model 11167, operating at intervals of about 300 meters (1000 feet) beginning at a depth of about 1200 meters (4000 feet). Table 1 gives the operating depth of each seismometer.

Table 1. Operating depths of the vertical array elements

Instrument	Operating depth prior to June 1967		Operating depth after February 1968	
	Meters	Feet	Meters	Feet
DH6	1191	3907	1190	3903
DH5	1494	4901	1493	4897
DH4	1796	5894	1792	5880
DH3	2106	6910	2102	6896
DH2	2409	7903	2405	7889
DH2	2711	8895	2707	8880

A block diagram of the system for a single instrument is shown in figure 3. The deep-hole seismometers have an undamped natural frequency of 1 cps, and their outputs are amplified by Model 4300 phototube amplifiers using 5 cps galvanometers. A typical deep-hole system amplitude response is shown in figure 4. In the period range of interest, 0.5 to 2.0 seconds, the individual amplitude responses are generally within 10 percent of the typical amplitude response.

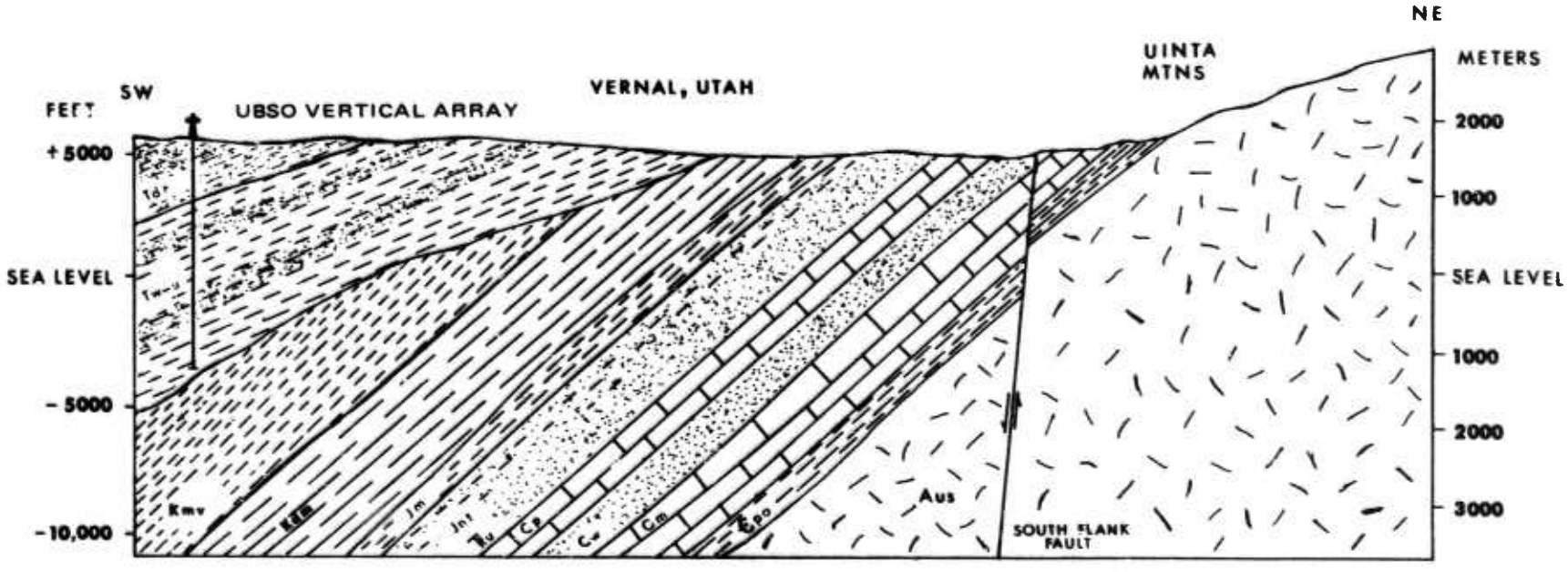

Tertiary	Tdr - Duchense River Tw-u - Wasatch - Green River - Uinta Gr.	
Cretaceous	Kmv - Mesa Verde Kdm - Dakota - Mancos	
Jurassic	Jmo - Morrison Jnt - Nugget - Twin Creek	
Triassic	Undivided	
Permian	Cp - Park City	
Pennslyvanian	Cw - Weber	
Mississippian	Cm - Madison	
Cambrian	Cpo - Pine Valley - Ophir	
Algonkian	Aus - Uinta Series	

Hypothetical Cross-Section

Vernal, Utah

Figure 1. Hypothetical cross-section showing vertical array

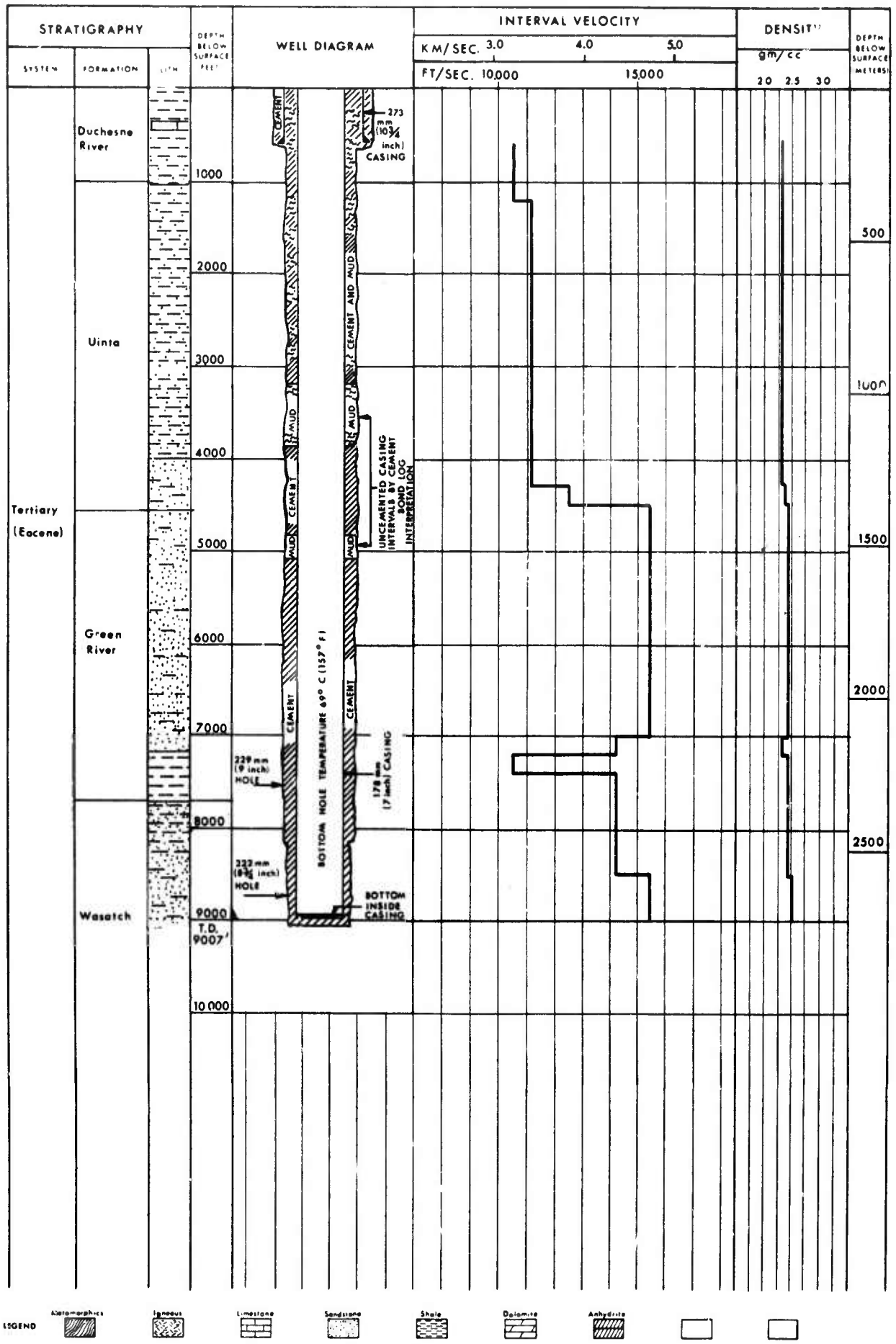

Figure 2. Log of the Carter U.S. No. 1 well at UBSO

G 4568

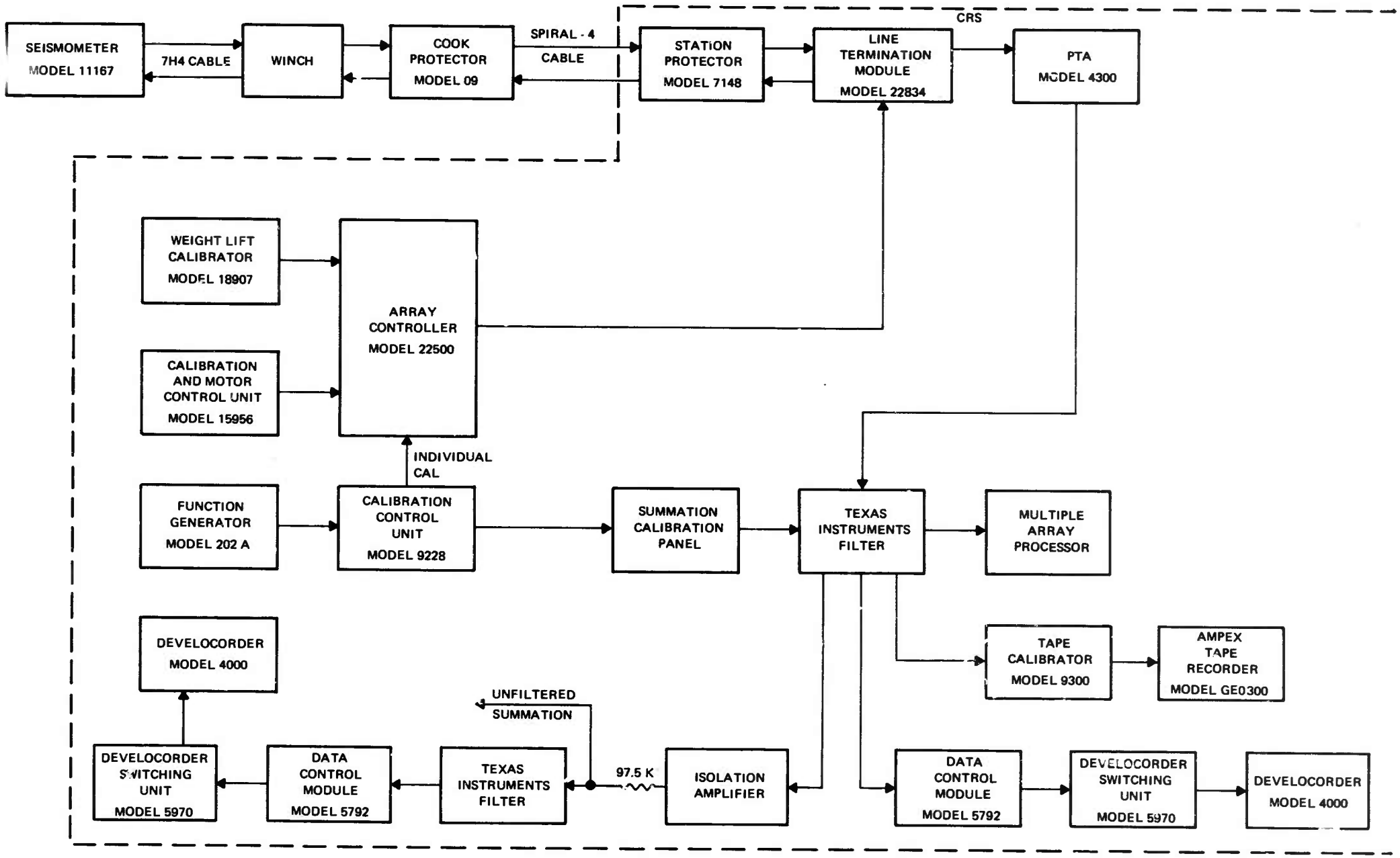

Figure 3. Block diagram of an individual deep-hole seismograph

G 4569

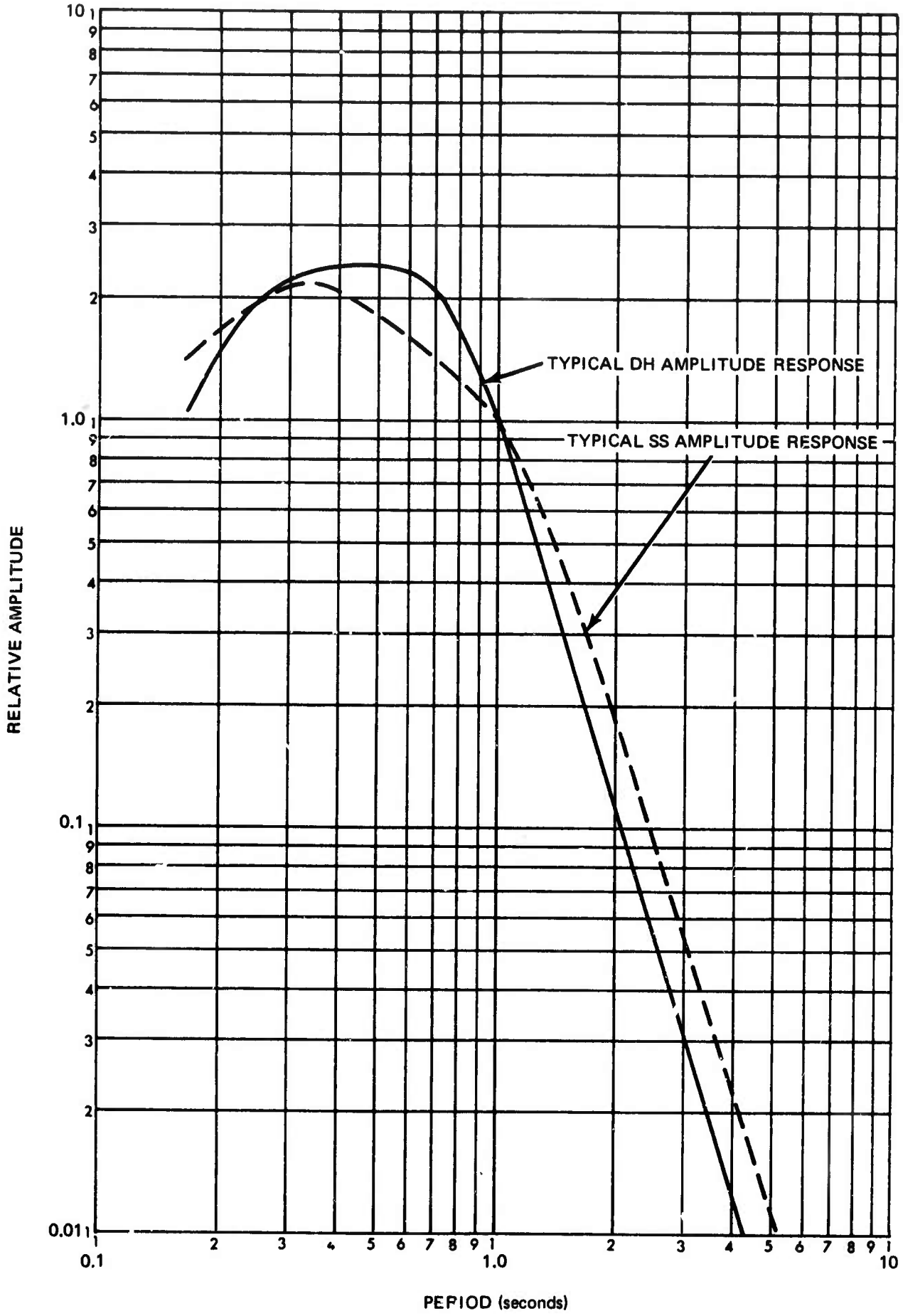

Figure 4. Vertical array and subsurface array amplitude response

G 4570

2.2 SUBSURFACE ARRAY

2.2.1 Array Geometry

The subsurface array consists of ten shallow borehole seismometers operating at a depth of about 200 feet. The configuration of the array is shown in figure 5. The location of the vertical array relative to the subsurface array is also shown.

2.2.2 System Response

The subsurface array system amplitude response is shown in figure 4. In comparison with the deep-hole response, periods greater than 1.5 seconds are attenuated less by about 5 dB. For the period range 0.3 to 1.0 second, the subsurface response is less than the deep-hole response.

3. DATA ENSEMBLE

3.1 DATA SELECTION

For the evaluation of the vertical array and comparison to the subsurface array, four signals and two noise samples were selected. Each noise sample is associated with two signals recorded on the same day. The location of the epicenter, magnitude, and other pertinent data for each signal are listed in table 2.

Figures 6 and 7 show the initial arrival of each of the signals as they were recorded by DH1 through DH6, the summation of the deep-hole outputs (ΣDH), SZ1, and the summation of the subsurface outputs (ΣSS). The ΣSS was not selected for the data ensemble on signals 1 and 2 due to low recording level on FM magnetic tape. For each signal, all the seismograph outputs have been normalized to the same magnification at 1.0 cps.

3.2 DATA PREPARATION

The signal and noise samples were digitized at a rate of 25 samples per second from FM magnetic tape. Prior to digitization, the data were filtered with a band-pass filter with cutoff frequencies at 0.1 and 6.0 cps. The cutoff rates were 18 and 24 dB/octave, respectively. Compensation for wow and flutter noise was made during playback. Calibrations for each seismograph for each day were also digitized.

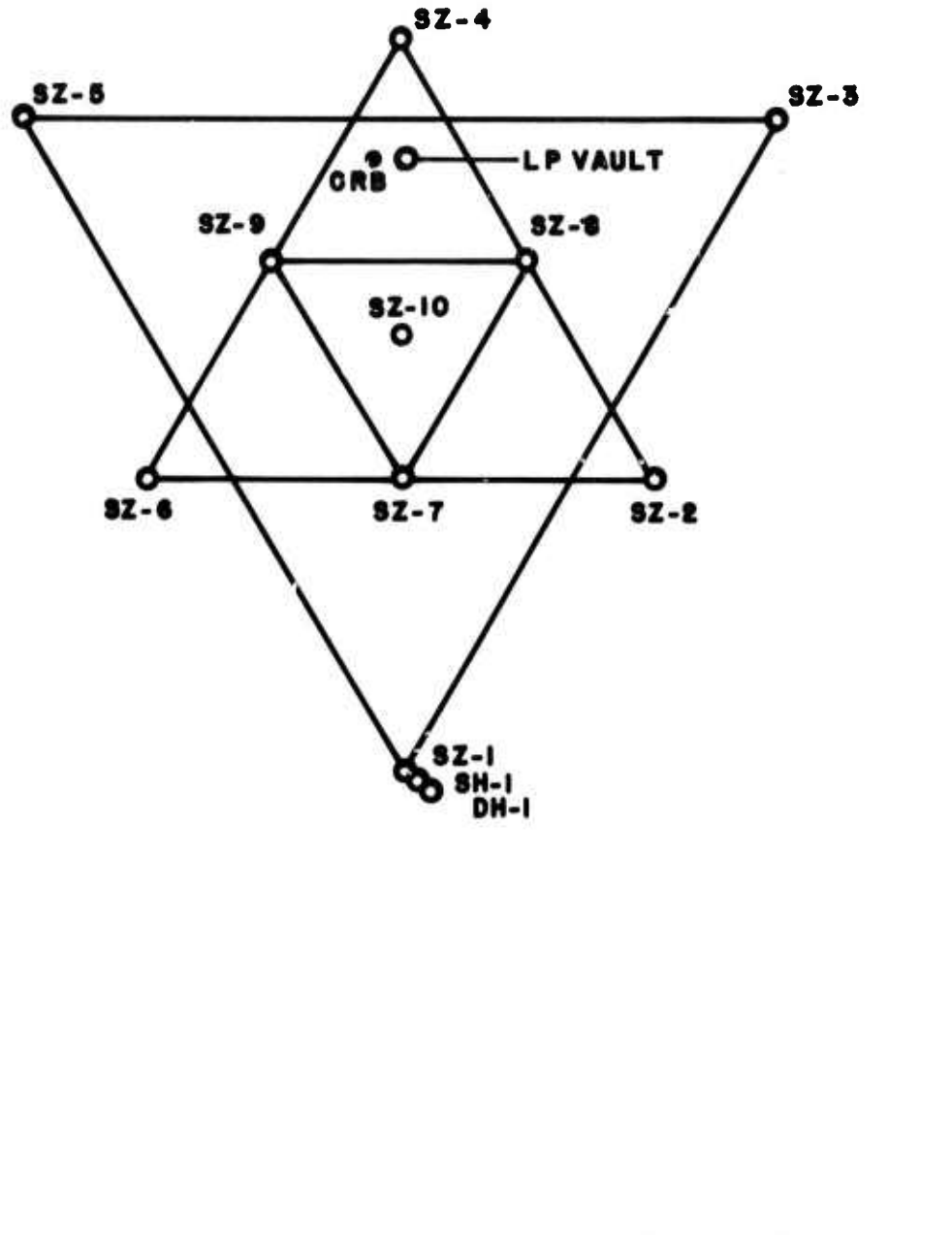

Figure 5. Orientation and configuration of UBSO arrays

Table 2. Epicenter data for four signals

Signal	Date	Origin time (Z)	Lat.	Long.	Region	Mag.	Depth	Distance (degrees)	Approx. angle of incidence (degrees)
1	1 Feb 1967	14:44:07.7	16.7S	72.7W	Peru	4.9	41K	66.3	25
2	1 Feb 1967	15:19:56.8	4.8S	103.2E	Sumatra	5.3	33K	134.0	5
3	21 Apr 1968	09:24:35.5	23.4S	70.5W	Chile	5.5	41K	69.1	20
4	21 Apr 1968	14:44:06.3	54.9N	161.5E	Kamchatka	4.6	28K	61.4	25

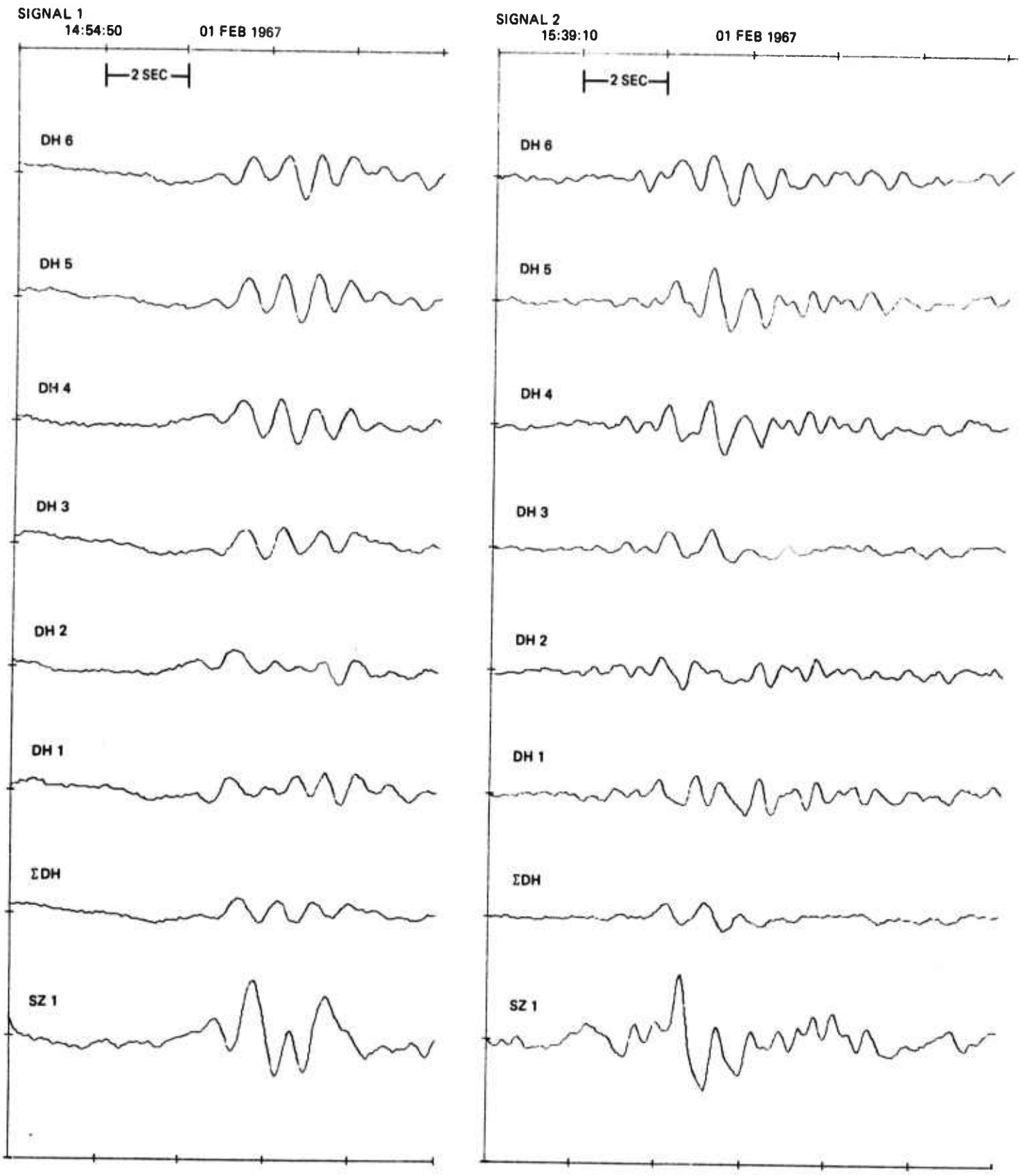

Figure 6. Initial arrivals for signals 1 and 2

G 4571

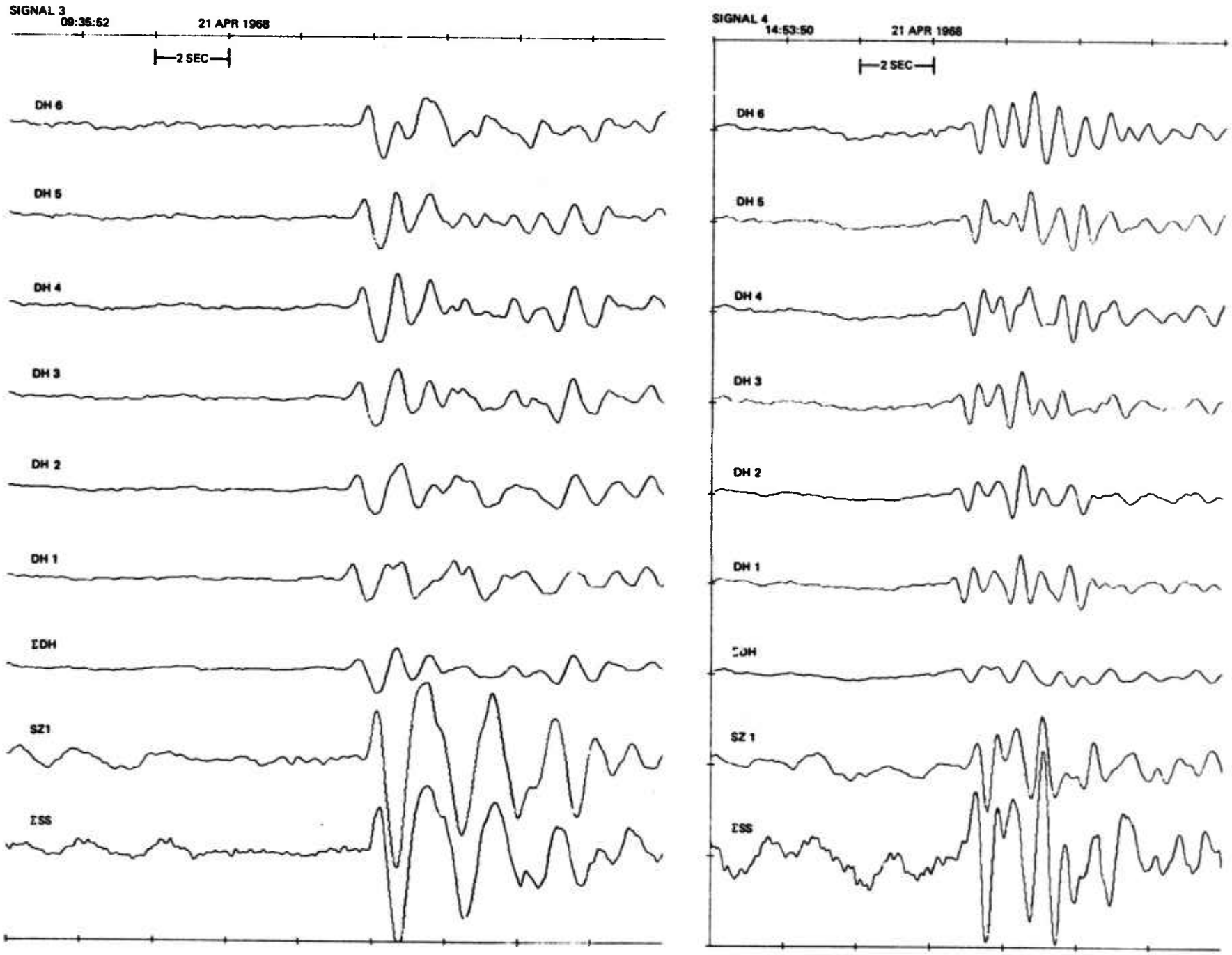

Figure 7. Initial arrivals for signals 3 and 4

G 4672

4. DATA ANALYSIS

4.1 SIGNAL-TO-NOISE RATIOS

Signal-to-noise ratio was computed by taking the ratio of one-half the peak peak-to-peak signal amplitude to the rms of the noise. The signal amplitude was measured on the largest half cycle in the first few seconds of the signal. The rms noise value was computed for the period range 0.5 to 2.0 seconds for a 3-minute, 25-second sample.

For the two signals for which the subsurface summation seismograph was available, the individual deep-hole elements provided slightly better signal-to-noise ratios. The subsurface summation did not show any significant improvement in S/N over SZ1. This should be tempered with the fact that only 2 signals were considered.

Table 3 gives the rms values for each seismograph for both noise samples. The difference of about 10.5 dB between the rms noise values of the deep-hole and subsurface systems is due partly to the difference in the system amplitude responses at the longer periods. The deep-hole summation gives about 2 dB rms noise reduction, relative to the average of the deep-hole rms noise values.

Table 3. Rms noise values for two noise samples

Seismograph	1 Feb 1967 rms (mμ)	21 April 1968 rms (mμ)
DH1	0.34	0.19
DH2	0.35	0.20
DH3	0.34	0.21
DH4	0.33	0.26
DH5	0.35	0.24
DH6	0.39	0.31
ΣDH	0.27	0.19
SZ1	1.24	0.82
ΣSS	Not available	0.89

The maximum amplitudes (uncorrected for frequency response) for each signal as recorded by each seismograph are given in table 4.

Table 4. Signal amplitudes for four signals

Seismograph	Signal 1 (p-p)/2 (mμ)	Signal 2 (p-p)/2 (mμ)	Signal 3 (p-p)/2 (mμ)	Signal 4 (p-p)/2 (mμ)
DH1	2.98	3.50	4.29	5.58
DH2	2.33	2.91	5.79	6.08
DH3	2.92	3.12	6.55	6.51

Table 4, Continued

Seismograph	Signal 1 (p-p)/2(mμ)	Signal 2 (p-p)/2 (mμ)	Signal 3 (p-p)/2 (mμ)	Signal 4 (p-p)/2 (mμ)
DH4	4.18	5.05	7.87	5.34
DH5	4.45	5.84	6.47	6.10
DH6	4.16	4.59	5.90	8.18
ΣDH	2.24	2.71	5.16	2.26
SZ1	8.80	10.75	20.94	9.32
ΣSS	--	--	18.38	13.88

The data for each signal have been normalized to the same magnification. Due to the constructive addition of the surface reflection, the upper deep-hole instruments generally show larger amplitudes than the lower instruments. Table 5 gives the signal-to-noise ratio (S/N) for each signal and the S/N improvement in dB relative to SZ1. The data indicate that the individual deep-hole seismographs can provide significant (5-8 dB) S/N improvement over the individual subsurface seismograph. However, for one of the signals there was no essential difference in S/N for the two systems. It should be noted that some of the improvement is due to the difference in system amplitude responses.

The deep-hole summation seismograph does not compare favorably with the individual deep-hole seismographs. The summation suffers because the surface reflection causes the signal to look different on each deep-hole seismograph.

4.2 NOISE ANALYSIS

4.2.1 UBSO Model

The basic method of noise analysis consisted of comparing experimental and theoretical ratios of amplitudes at various depths to amplitudes at the surface for several wave types. The basis for determining the theoretical ratios for Rayleigh waves was a layered model derived from the velocity and density data presented in figure 2. Table 6 gives the thickness, P-wave velocity, S-wave velocity, and density of each layer.

4.2.2 Fundamental Mode Rayleigh Waves

The UBSO model was used to calculate the theoretical fundamental mode Rayleigh amplitude ratio, relative to the surface, at each of the depths where a deep-hole instrument was located. These calculations were made for the period range 2.0 to 6.0 seconds, with a period increment of 0.05 seconds. Amplitude ratios for one deep-hole seismograph relative to another deep-hole seismograph were obtained from the deep-hole relative to surface ratios.

Table 5. Signal-to-noise ratios and improvement factors relative to SZ1 for four signals

	Signal 1		Signal 2		Signal 3		Signal 4	
Seismograph	S/N	S/N Improvement	S/N	S/N Improvement	S/N	S/N Improvement	S/N	S/N Improvement
DH1	8.76	1.8 dB	10.29	1.5 dB	22.58	-1.1 dB	29.37	8.2 dB
DH2	6.66	-0.6 dB	8.31	-0.4 dB	28.95	0.5 dB	30.40	8.5 dB
DH3	8.59	1.7 dB	9.18	0.5 dB	31.19	0.9 dB	31.00	8.7 dB
DH4	12.67	5.0 dB	15.30	4.9 dB	30.27	0.7 dB	20.54	5.2 dB
DH5	12.71	5.1 dB	16.69	5.7 dB	26.96	0.2 dB	25.42	7.0 dB
DH6	10.67	3.5 dB	11.77	2.7 dB	19.03	-2.6 dB	26.39	7.3 dB
ΣDH	8.30	1.4 dB	10.04	1.3 dB	27.16	0.3 dB	11.89	0.2 dB
SZ1	7.10	0.0 dB	8.67	0.0 dB	25.54	0.0 dB	11.37	0.0 dB
ΣSS	--	--	--	--	20.65	-1.9 dB	15.59	2.7 dB

Table 6. Seismic velocities for the UBSO geologic model

Thickness of layer (km)	P-wave velocity (km/sec)	S-wave velocity (km/sec)	Density (gm/cc)	Depth to top of layer (km)
0.18	2.8	1.6	2.30	0
0.19	3.2	1.8	2.30	.18
0.92	3.4	1.9	2.30	.37
0.06	3.8	2.1	2.35	1.29
0.75	4.6	2.6	2.40	1.35
0.07	4.4	2.5	2.30	2.10
0.08	3.2	1.8	2.40	2.17
0.32	4.4	2.5	2.40	2.25
0.13	4.7	2.7	2.50	2.57
38.0	6.0	3.4	2.60	2.70
∞	8.0	4.5	2.68	40.70

The experimental noise amplitude ratios were determined from power density spectra by taking the square root of the ratio of two deep-hole noise spectra. The noise amplitude ratios were computed at each period for which the spectra were computed. Since the system amplitude responses of the individual deep-hole elements are essentially identical, the experimental amplitude ratios are independent of the system response. The power spectra for the individual deep-hole seismographs, ΣDH, and SZ1 are shown for both noise samples in figures 8 through 11. The peak power recorded by the deep-hole systems, which occurs at a period between 5 and 6 seconds, is about 4 to 5 dB below the peak power on the subsurface system due to the difference in the system amplitude responses at the longer periods. A secondary peak in the noise spectra for both samples occurs in the period range 1.0 to 2.0 seconds.

The comparison between the theoretical fundamental mode Rayleigh amplitude ratios and the experimental noise amplitude ratios is shown in figures 12 through 15. Except for a possible magnification error in the ratio of DH1 to DH6 for noise sample 2 (21 April 1968), the agreement between the theoretical and the experimental ratios is very good. The data indicate that the noise, as recorded by the deep-hole system, consists of fundamental mode Rayleigh waves for periods greater than about 2.5 seconds.

4.2.3 P-Wave Noise

The theory for computing amplitude ratios for P-wave noise has been established (Geotech, TR 67-3). The basic assumptions used are the following:

1. P-wave noise arriving independently from all angles of incidence with equal energy content;

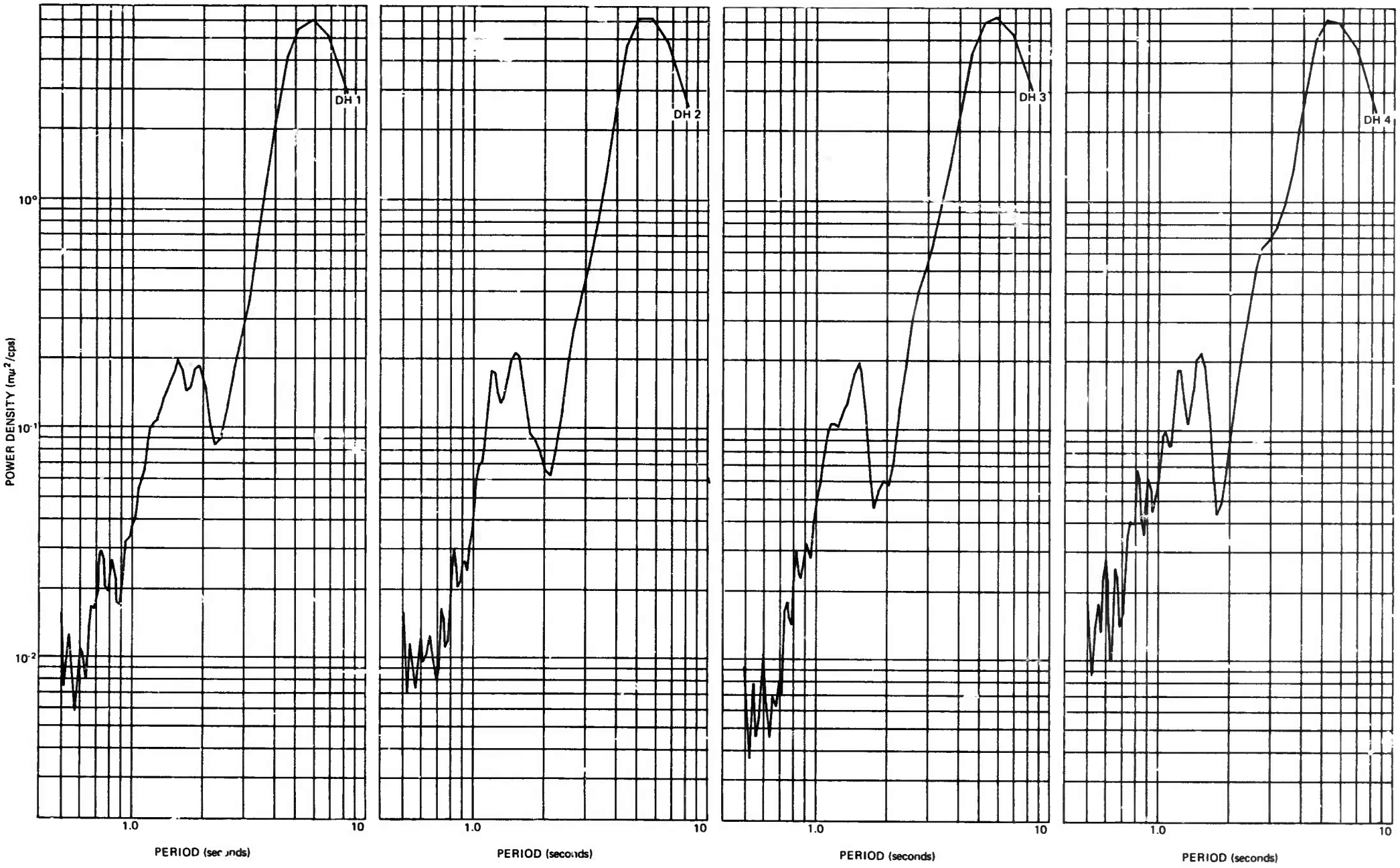

Figure 8. Power density spectra for noise sample 1 as observed on DH1, DH2, DH3, DH4

G 4573

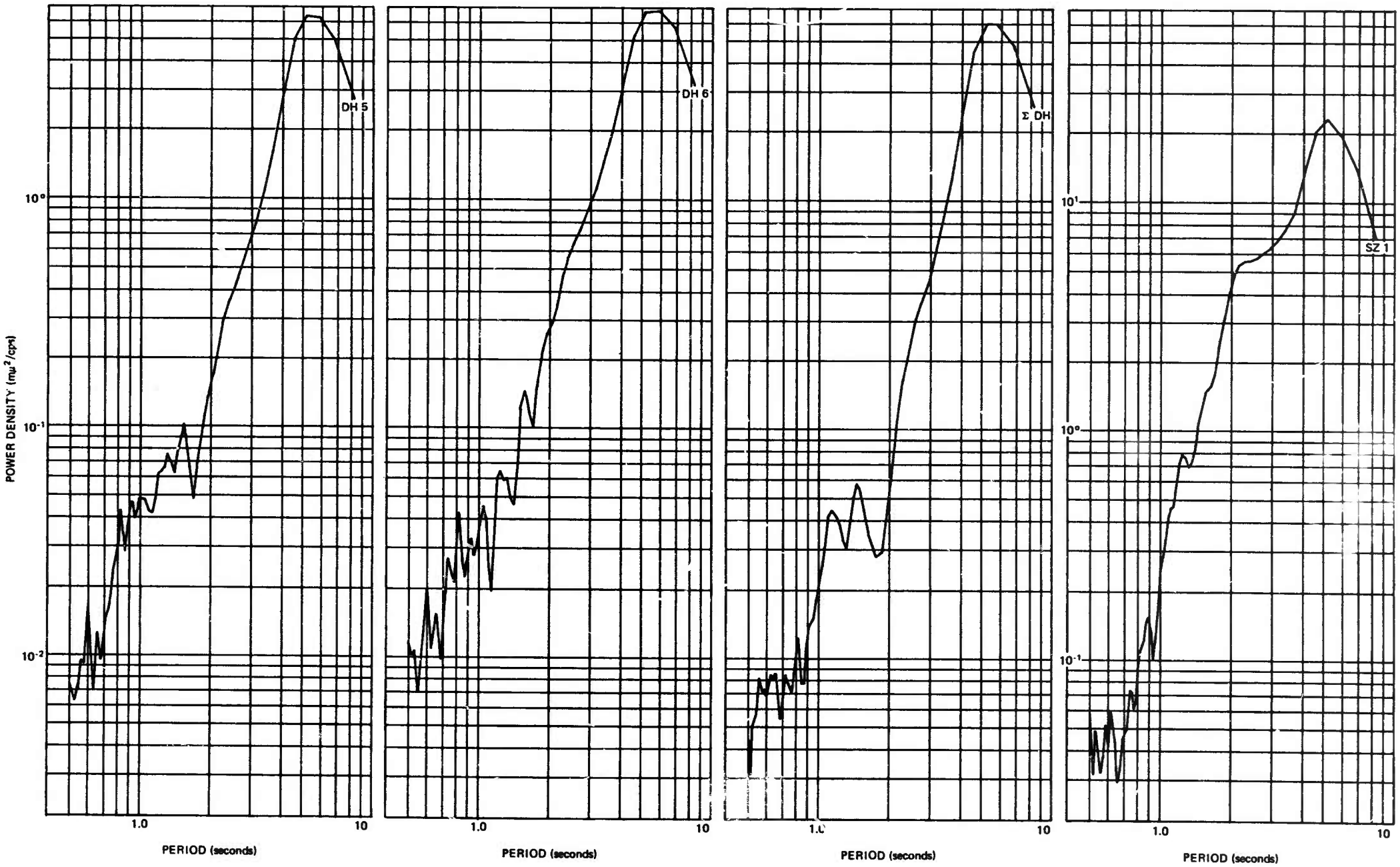

Figure 9. Power density spectra for noise sample 1 as observed on DH5, DH6, ΣDH, and SZ1

G 4574

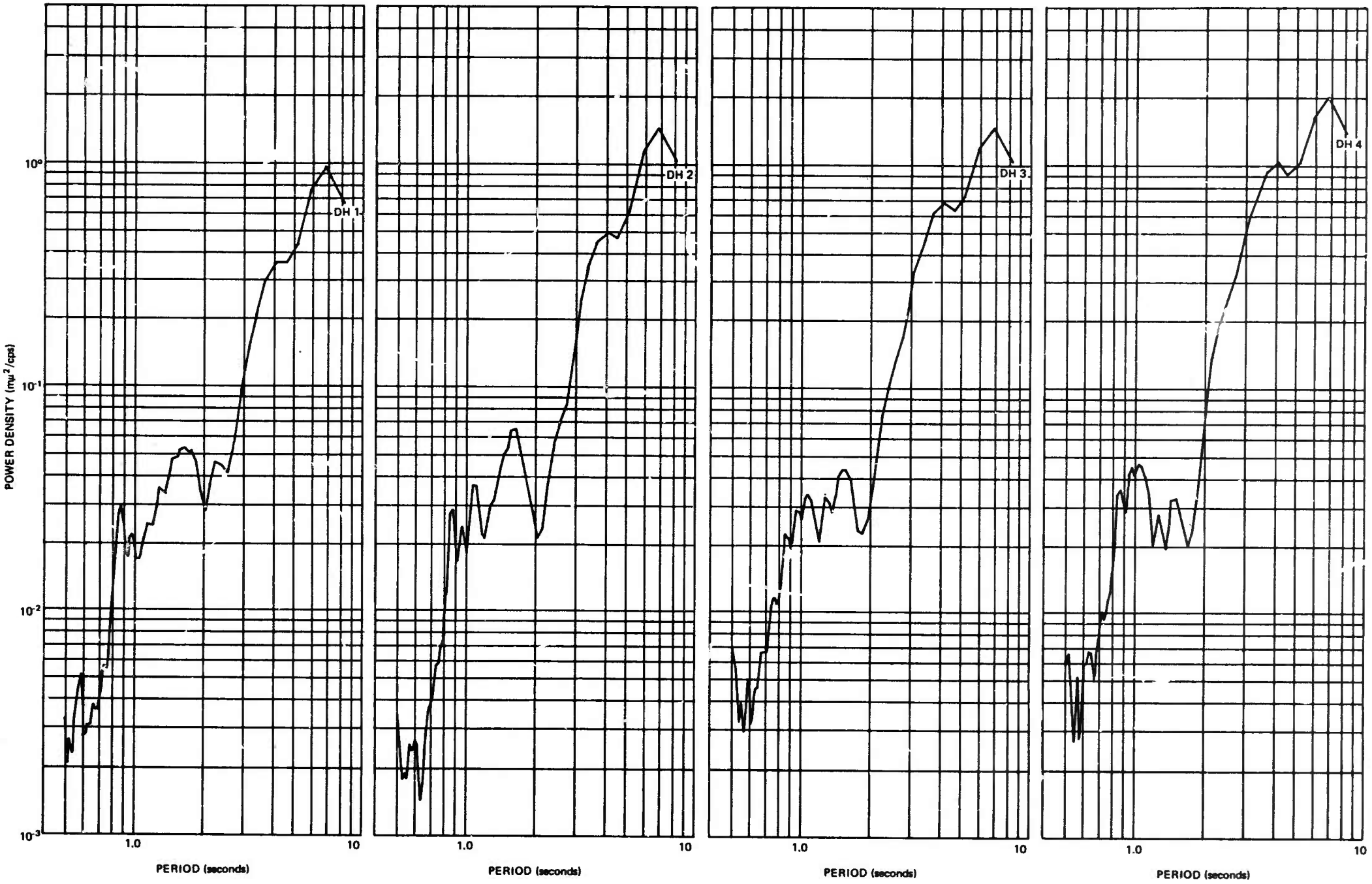

Figure 10. Power density spectra for noise sample 2 as observed on DH1, DH2, DH3, and DH4

G 4575

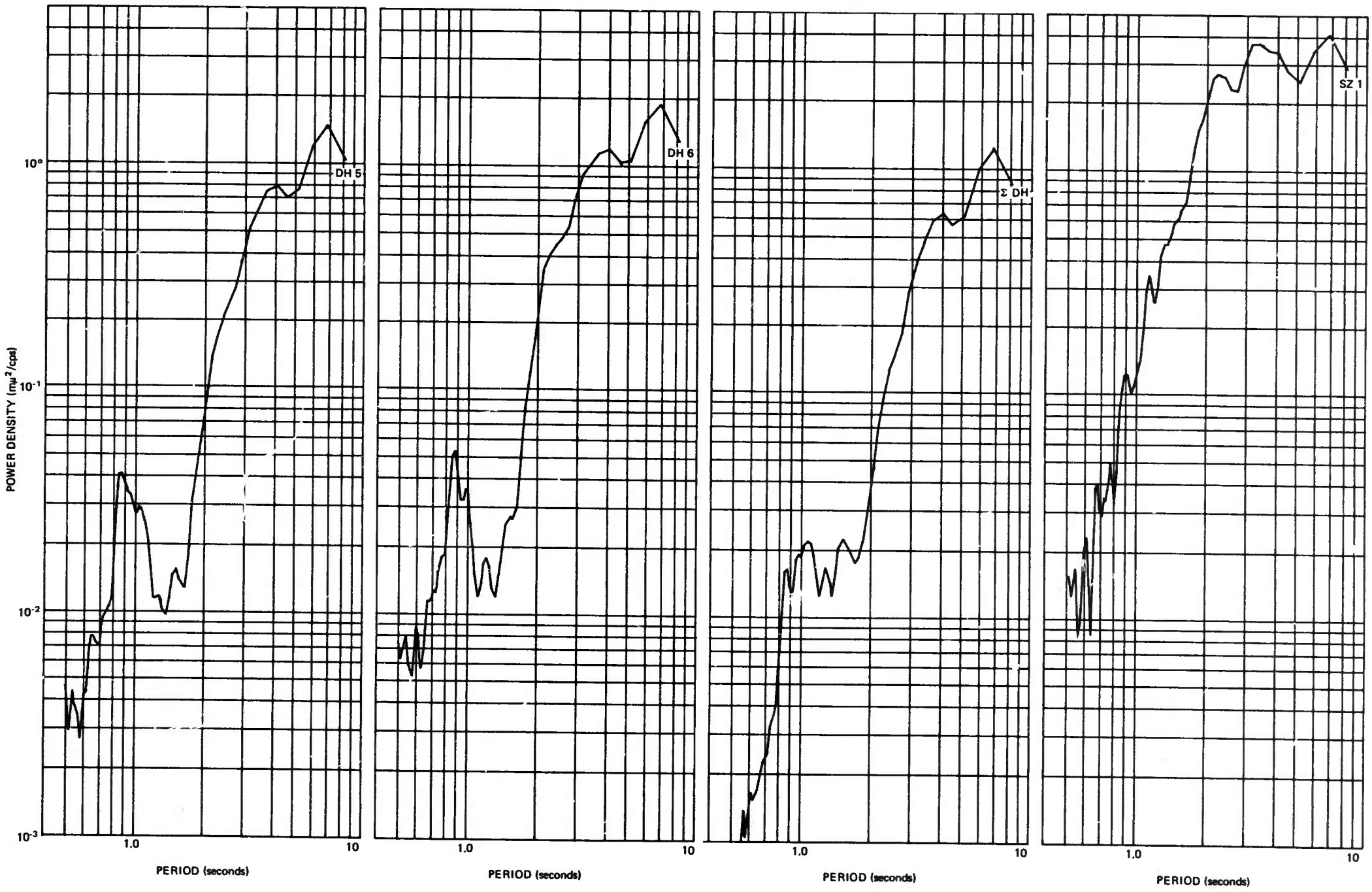

Figure 11. Power density noise spectra of noise sample 2 as observed on DH5, DH6, ΣDH, and SZ1

G 4576

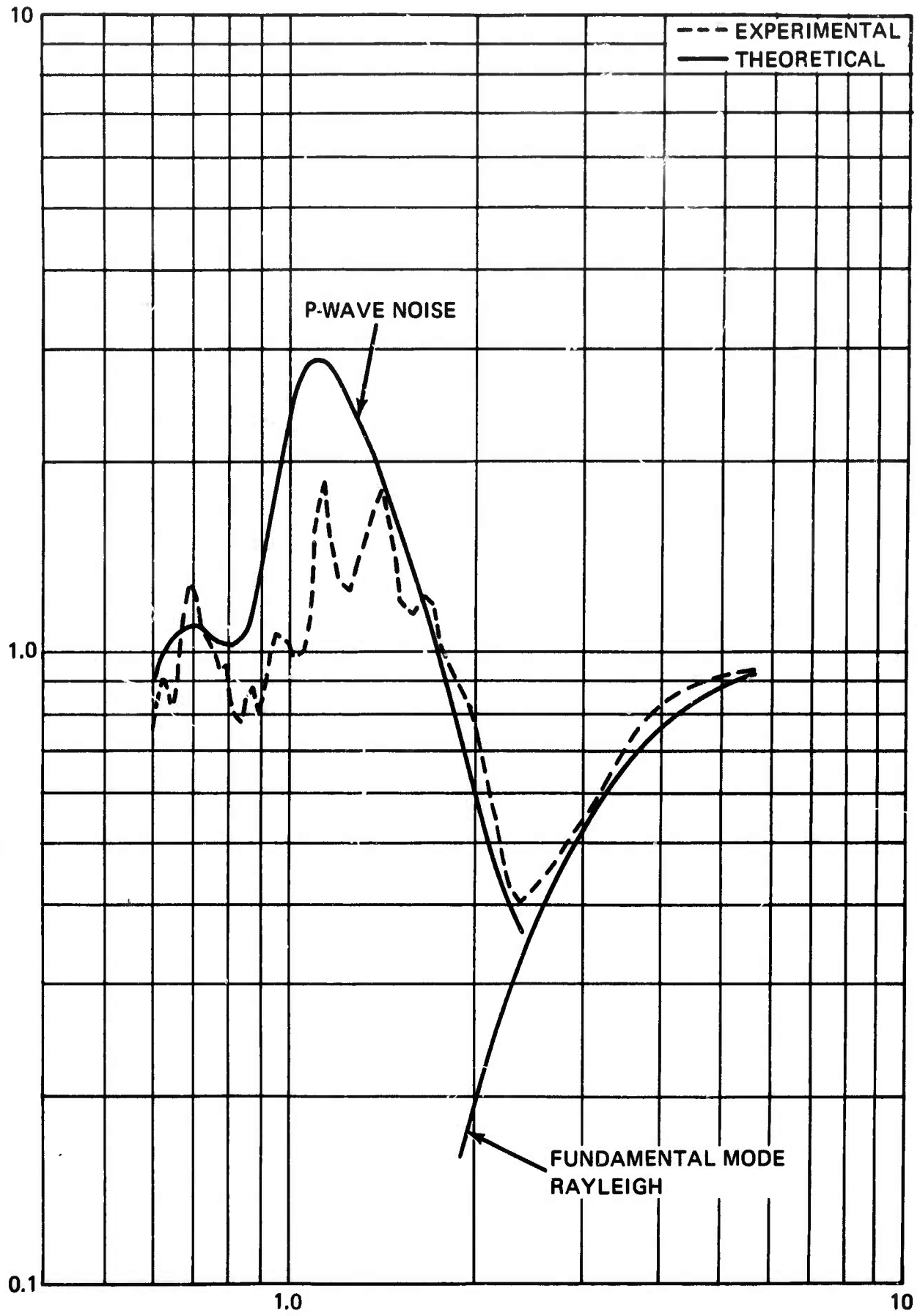

Figure 12. Experimental and theoretical noise amplitude ratios for DH1 and DH6

G 4577

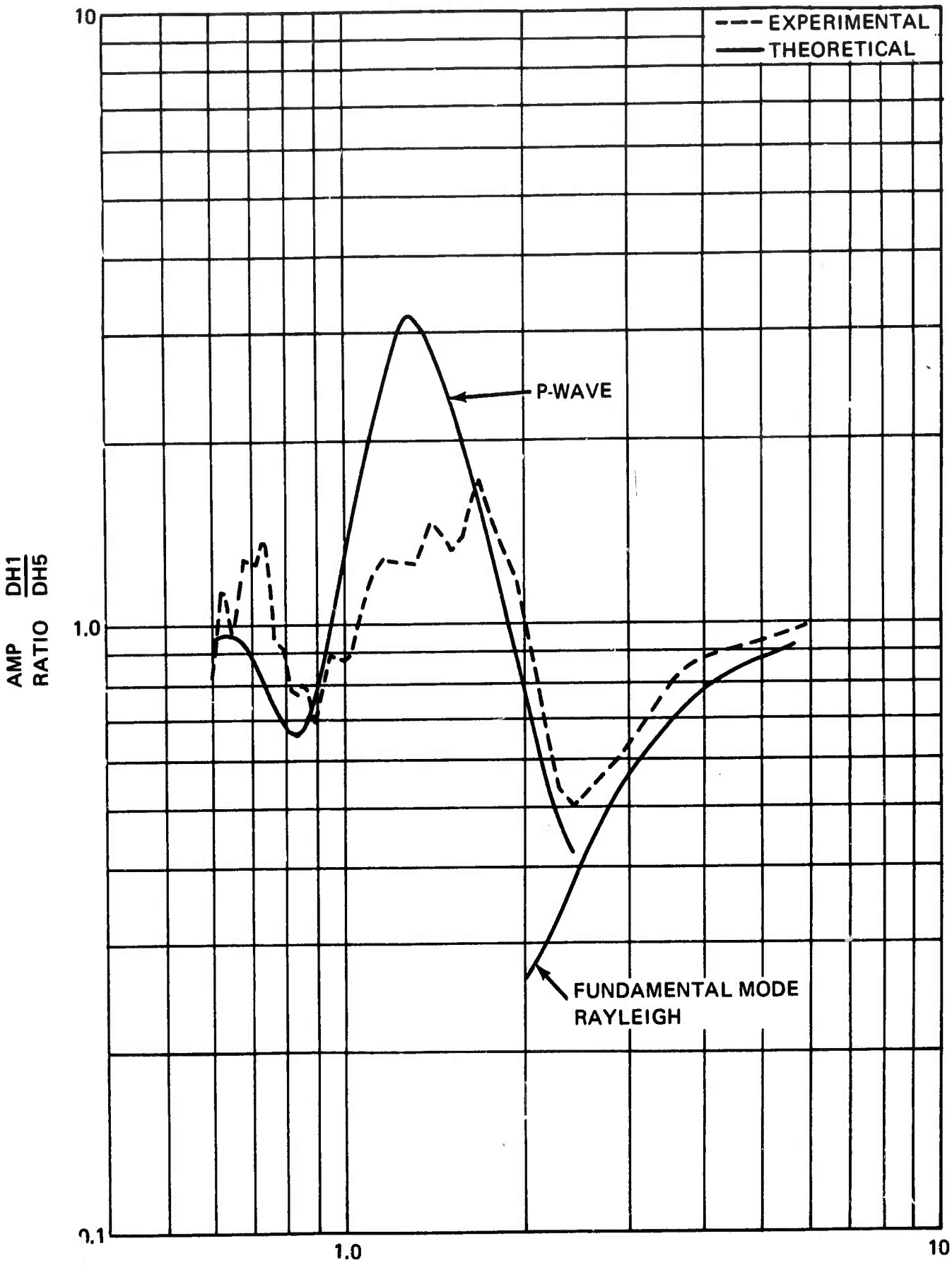

Figure 13. Experimental and theoretical noise amplitude ratios for DH1 and DH5

G 4578

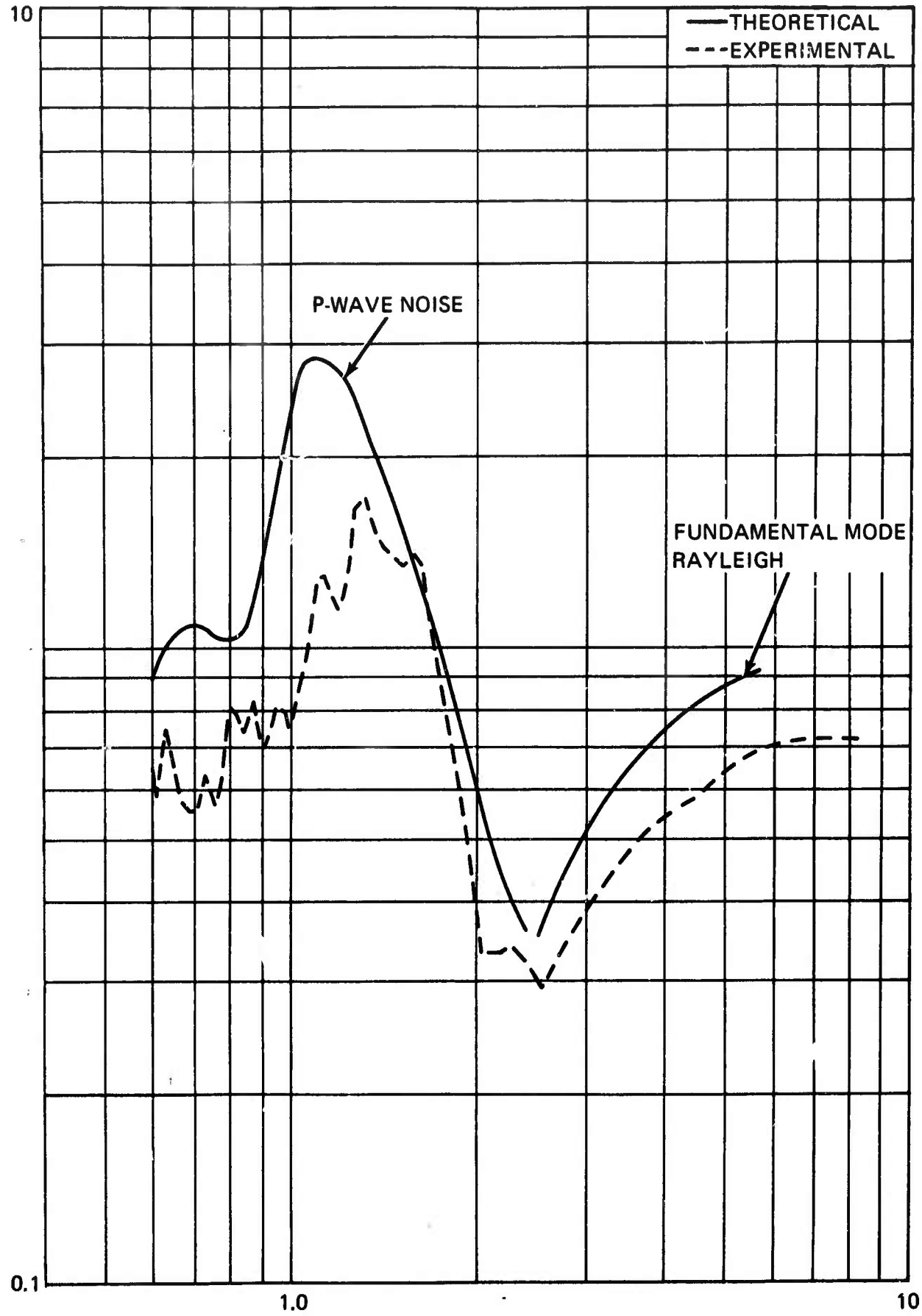

Figure 14. Experimental and theoretical noise amplitude ratios for for DH1 and DH6

G 4579

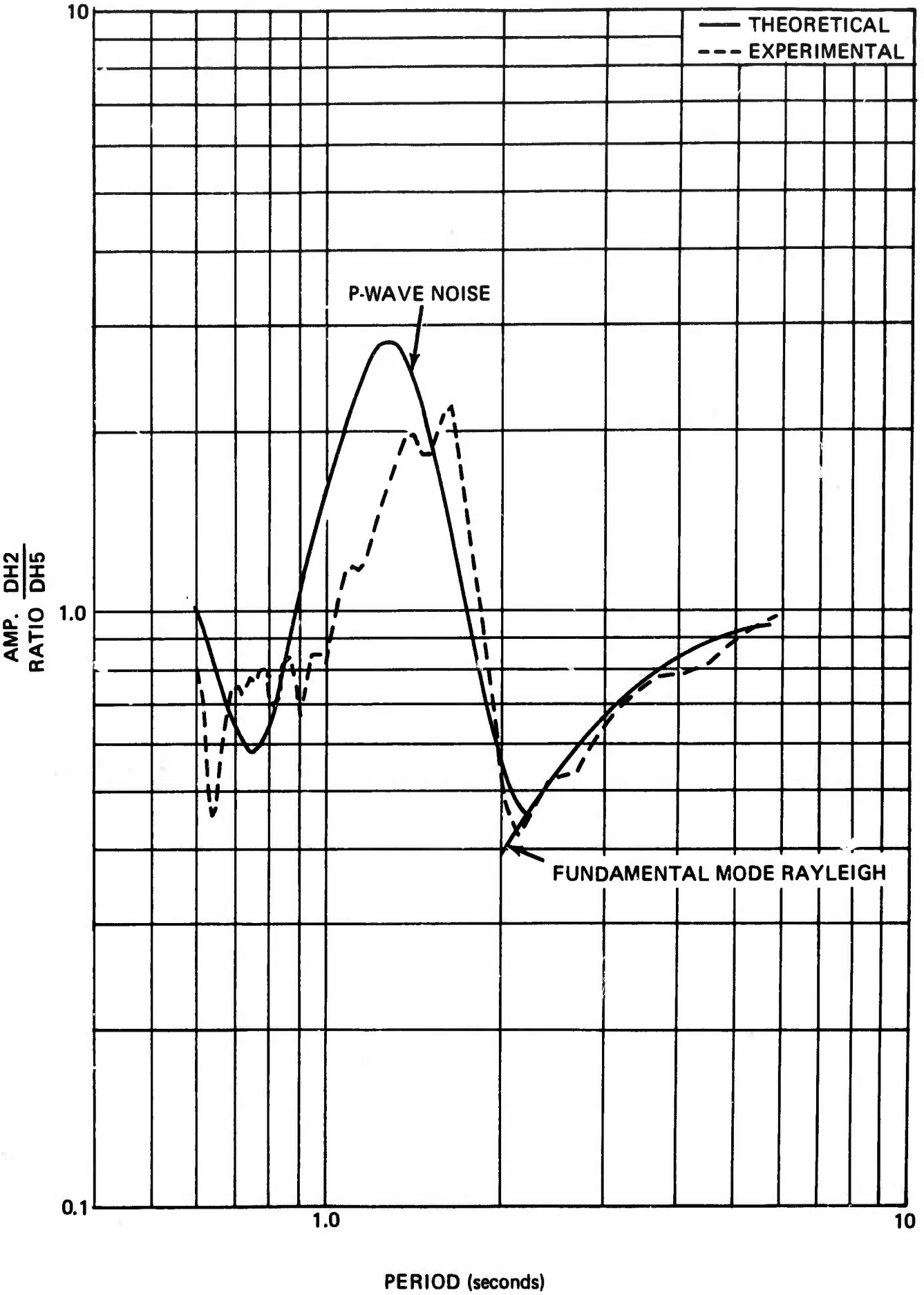

Figure 15. Theoretical and experimental noise amplitude ratios for DH2 and DH5

G 4580

2. No conversion from P to S waves at the free surface;

3. An isotropic, homogeneous half space.

The amplitude ratio for P-wave noise is given by the expression

$$\sqrt{\left(1/2 + J_o\ (\alpha_1\omega) - \frac{J_1(\alpha_1\omega)}{\alpha_1\omega}\right) \Big/ \left(1/2 + J_o\ (\alpha_2\omega) - \frac{J_1(\alpha_2\omega)}{\alpha_2\omega}\right)}$$

where J_o and J_1 are zero and first order Bessel functions, respectively, and α_i is twice the vertical uphole time from a depth d_i. The velocity for the halfspace was computed by weighting the velocity of each layer by the thickness of the layer. This resulted in an average velocity of 3.96 kilometers/second.

Figures 12 through 15 show the theoretical amplitude ratios in the period range 0.6 to 2.5 seconds. A comparison with the experimental noise amplitude ratios indicates that there is basic agreement in the overall trend. Particularly good agreement is evident from the figures for the period range of about 1.5 to 2.5 seconds. A trough at about 0.8 second is common to both the experimental and theoretical ratios for noise sample 1. The poorest agreement occurs in the period range of about 1.0 to 1.5 seconds. This behavior could be explained by either of the following:

1. There is another wave-type in this period range which is not completely dominated by P-wave noise.

2. The model is too simple to adequately represent the noise behavior. It should be noted that the agreement could be improved in the period range 1.0 to 1.5 seconds without degrading the agreement at other periods by using a slightly smaller P-wave velocity.

The theoretical coherence for P-wave noise based on the assumptions made in calculating the theoretical P-wave amplitude ratios is given by the equation

$$\text{coherence} = \frac{\left| \frac{J_o\left(\frac{\omega\ (\alpha_1+\alpha_2)}{2}\right)}{2} - \frac{J_1\left(\frac{\omega\ (\alpha_1+\alpha_2)}{2}\right)}{\omega\ (\alpha_1+\alpha_2)} + \frac{J_o\left(\frac{\omega\ (\alpha_1-\alpha_2)}{2}\right)}{2} - \frac{J_1\left(\frac{\omega\ (\alpha_1-\alpha_2)}{2}\right)}{\omega\ (\alpha_1-\alpha_2)} \right|}{\sqrt{\left(1/4 + \frac{J_o\ (\alpha_1\omega)}{2} - \frac{J_1\ (\alpha_1\omega)}{2\alpha_1\omega}\right)\left(1/4 + \frac{J_o\ (\alpha_2\omega)}{2} - \frac{J_1\ (\alpha_2\omega)}{2\alpha_2\omega}\right)}}$$

The theoretical and experimental (noise sample 2) coherence between DH1 and DH6 is shown in figure 16. Noise sample 2 was used for this comparison because the agreement between the amplitude ratios for this sample (figure 14) was better than the agreement between amplitude ratios observed for noise sample 1 (figure 12). The troughs at about 1.0 and 2.25 seconds and the peak at about 1.5 seconds on the experimental coherence function are in good agreement with the theoretical curve.

4.3 SIGNAL ANALYSIS

The UBSO layered model was used for theoretical computation of the relative deep-hole P-wave amplitudes for each of the four signals. For the given model, the theoretical values depend on the frequency and the angle of incidence of the signal. The angles of incidence used are given in table 2. The frequencies selected for comparison of theoretical and experimental values were dominant frequencies in the signal.

The experimental relative signal amplitudes for a given period were determined from power density spectra. Figures 17 and 18 show the comparison between the experimental and the theoretical relative amplitudes. For the periods compared, the experimental values follow the trend of the theoretical curves, suggesting that the signals behave basically as the model predicts. Because of this agreement, the model was used to predict the deep-hole element which could be expected to record the largest signal amplitudes from a 1 cps teleseismic signal. Figure 19 shows the theoretical signal amplitude, relative to SZ1, for each deep-hole element as a function of angle of incidence. The theoretical curves show that DH4 and DH5 are best situated to record 1.0-second signal amplitudes and that DH1 is generally the poorest element at this period. Note that for signals with periods greater than 1.0 second, the performance of DH1 is considerably improved, relative to the other deep-hole elements.

5. CONCLUSIONS

The analysis of the vertical array and subsurface array data ensemble suggests the following tentative conclusions:

a. The individual vertical array elements can provide significant (as much as 8 dB) improvement in S/N relative to an individual subsurface element.

b. The S/N of the vertical array summation does not compare favorably with the S/N of the individual deep-hole elements.

c. The ambient noise field, as seen through the vertical array, consists of fundamental mode Rayleigh waves for periods greater than 2.5 seconds. For periods less than 2.5 seconds, the predominant wave type appears to be P-wave noise.

d. There is basic agreement between observed and theoretically-predicted signal amplitudes as a function of depth.

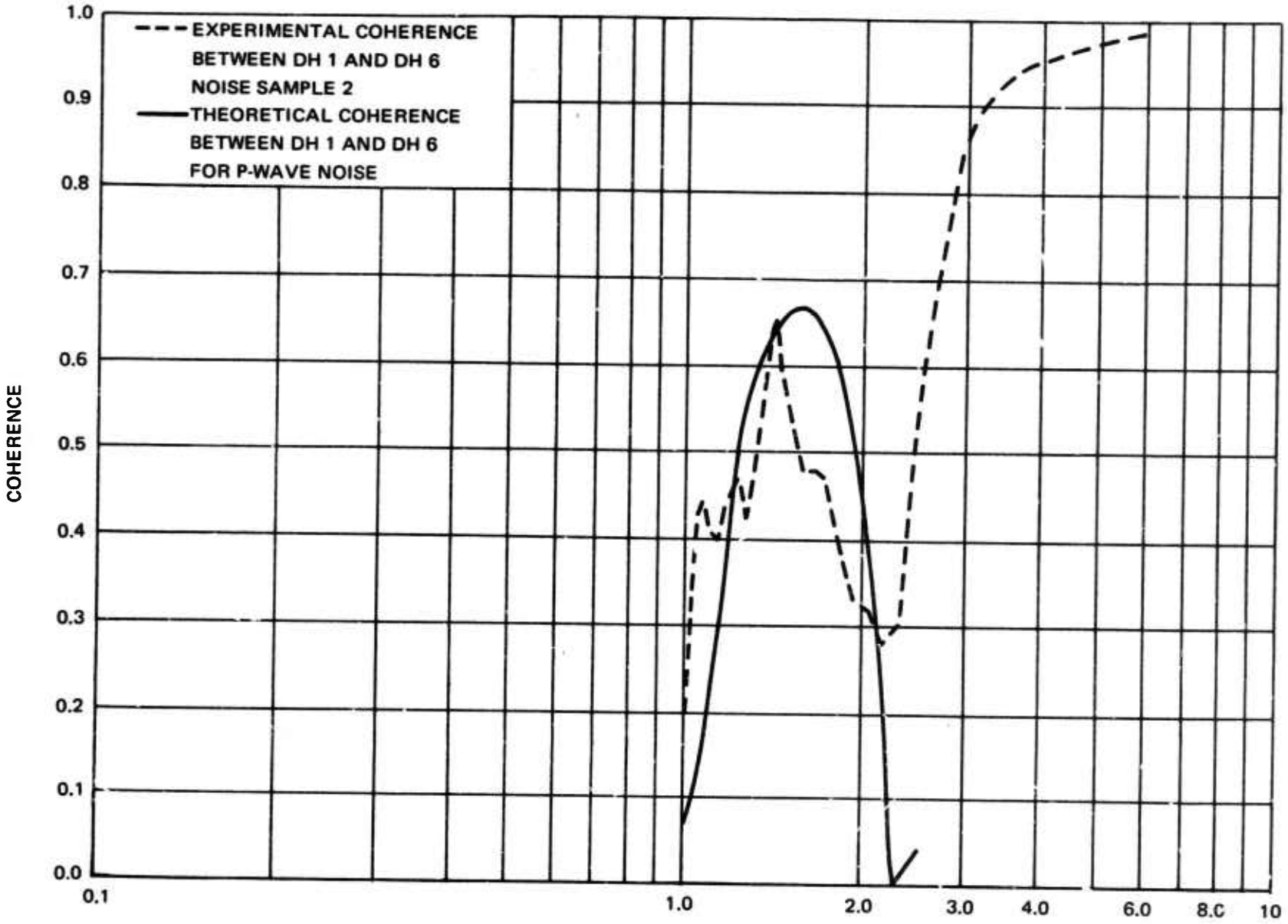

Figure 16. Theoretical and experimental coherence for DH1-DH6

G 4581

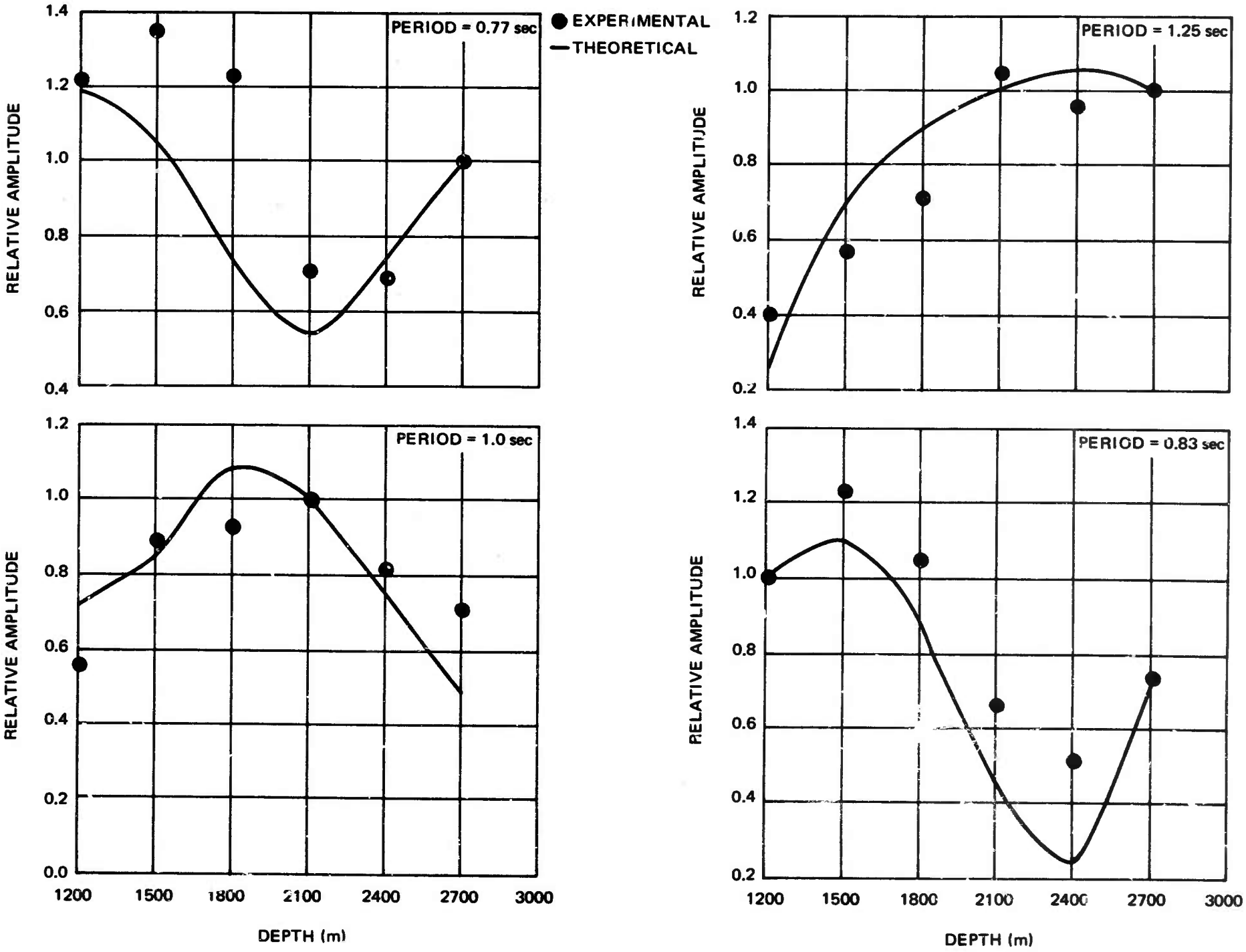

Figure 17. Experimental and theoretical P-wave amplitude-depth ratios

G 4582

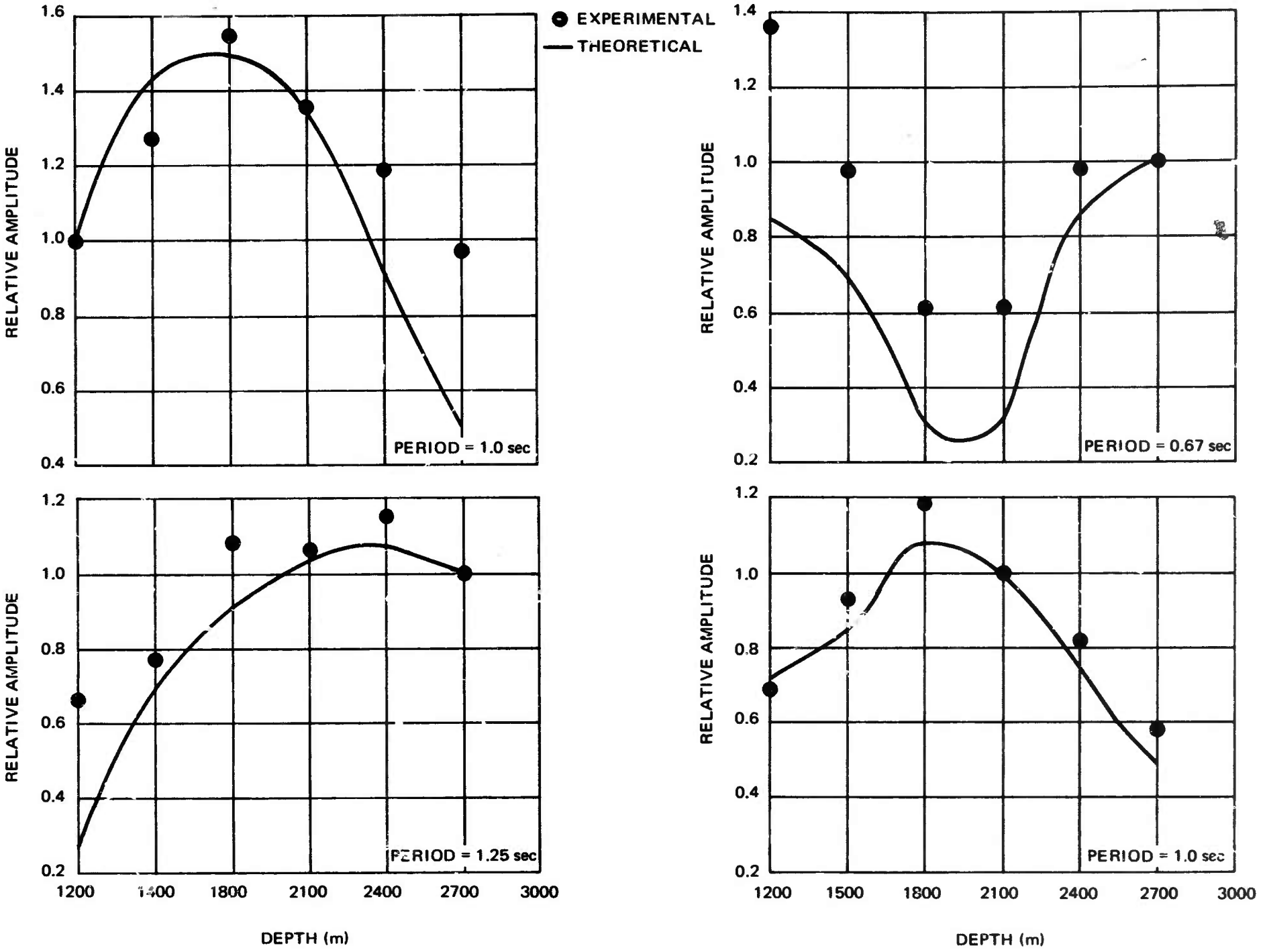

Figure 18. Experimental and theoretical P-wave amplitude-depth ratios

G 4583

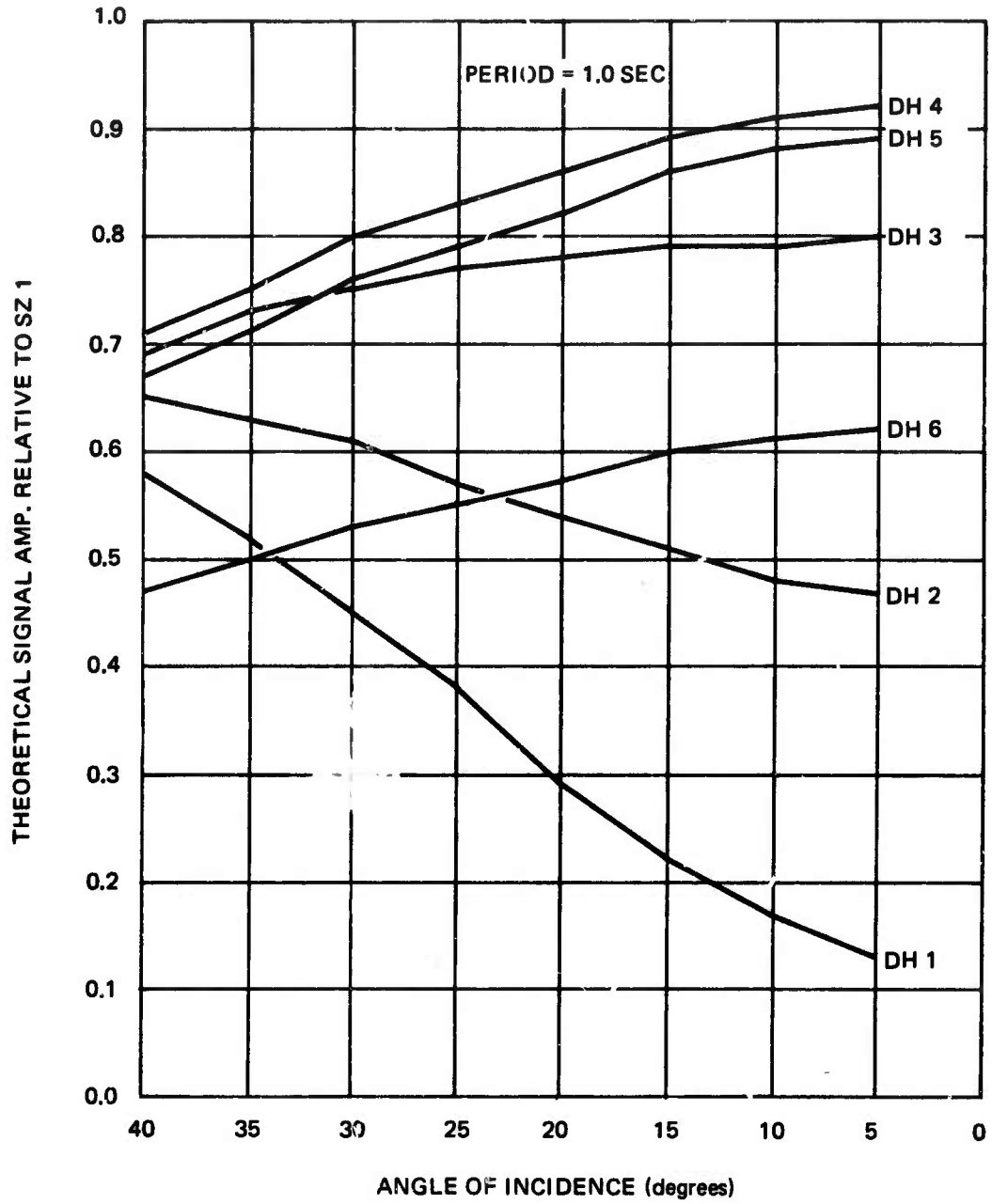

Figure 19. Theoretical P-wave amplitudes (relative to SZ1) as a function of angle of incidence

G 4584

6. RECOMMENDATIONS

This preliminary evaluation of the deep-hole system shows that further work is needed on the following tasks:

a. Determine a firm estimate of the signal-to-noise ratio improvement provided by the deep-hole system relative to the subsurface system.

b. The theory predicts, from the UBSO layered model, that DH4 and DH5 are the best situated elements to record 1.0-second signal amplitudes. Additional signals should be studied in order to empirically verify the optimum depths.

c. The collection of data for the evaluation of the vertical array was hampered by the unreliability of the vertical array seismographs. In order that the above studies may be implemented, we recommend that the present system be replaced with a more reliable system.

Unclassified
Security Classification

DOCUMENT CONTROL DATA - R & D

(Security classification of title, body of abstract and indexing annotation must be entered when the overall report is classified)

1. ORIGINATING ACTIVITY *(Corporate author)*
Geotech, A Teledyne Company
3401 Shiloh Road
Garland, Texas

2a. REPORT SECURITY CLASSIFICATION
Unclassified

2b. GROUP

3. REPORT TITLE
Preliminary Evaluation of the UBSO Vertical Array

4. DESCRIPTIVE NOTES *(Type of report and inclusive dates)*

5. AUTHOR(S) *(First name, middle initial, last name)*
Dale S. Kelley

6. REPORT DATE
16 December 1968

7a. TOTAL NO. OF PAGES
38

7b. NO. OF REFS

8a. CONTRACT OR GRANT NO.
AF 33(657)-16563

b. PROJECT NO.
VELA T/6705

c. ARPA Order No. 624
ARPA Program Code No. 6F10

d.

9a. ORIGINATOR'S REPORT NUMBER(S)
TR 68-51

9b. OTHER REPORT NO(S) *(Any other numbers that may be assigned this report)*

10. DISTRIBUTION STATEMENT
This document is subject to special export controls and each transmittal to a foreign national may be made only with prior approval of the Chief of AFTAC

11. SUPPLEMENTARY NOTES

12. SPONSORING MILITARY ACTIVITY
Advanced Research Projects Agency
Nuclear Test Detection Office
Washington, D. C.

13. ABSTRACT
The vertical array at the Uinta Basin Seismological Observatory consists of six short-period seismographs distributed along the 9000-foot depth of the Carter U. S. No. 1 well. A study of four data samples containing teleseismic earthquake signals indicated a maximum improvement of about 9 dB in signal-to-noise ratio of a single vertical array instrument to a surface instrument. Analyses of two noise samples indicate that the noise field consists of fundamental mode Rayleigh waves for periods greater than 2.5 seconds, at shorter periods the noise field is primarily dominated by P-wave noise.

DD FORM 1 NOV 65 1473

Unclassified
Security Classification

14. KEY WORDS	LINK A		LINK B		LINK C	
	ROLE	WT	ROLE	WT	ROLE	WT
Fundamental mode Rayleigh wave						
P-wave noise						
Signal-to-noise ratio improvement UBSO ambient noise field						